УДК 536.46

F. Aguerre, N. Darabiha, J. C. Rolon, S. Candel

EXPERIMENTAL AND NUMERICAL STUDY OF TRANSIENT LAMINAR COUNTERFLOW DIFFUSION FLAMES

Laboratoire EM2C, CNRS,
Ecole Centrale Paris,
92295 Chatenay-Malabry cedex, France

Abstract

In the present article, we analyze the nonsteady behaviour of counterflow diffusion flames submitted to a time dependent injection velocity in the case of hydrogen — air flames. The numerical study, using a finite difference implicit Linear Multistep Method and employing complex kinetics, is done for sinusoidal injection velocity variations, for moderate values and also for values near the extinction limit. The frequency response is obtained in these different cases. The experimental setup comprises two axisymmetric nozzles. In order to change the inlet velocities periodically, we use a vibrating mechanism in each burner. The amplitude and the frequency of injection velocities of the opposed nozzles are synchronously modified. The OH radical emission intensity is used to measure the flame response to velocity fluctuations. The experimental results are compared to numerical calculations. A good concordance is obtained in this comparison.

Introduction

The laminar counterflow configuration makes possible the study of the influence of different parameters on the flame structure using complex chemistry. The study can also be done experimentally. These flames constitute a basic component of flamelet models of turbulent combustion. In these models the local structure of the reaction zone is depicted as an ensemble of strained laminar flame elements which are stretched and convected by the turbulent flow. Because each flamelet spends a finite residence time in a given region of the turbulent field, it may not be able to adjust to the local conditions and reach the steady-state structure. The steady-state laminar counterflow flames have been extensively studied by theoretical methods [1—9] and experimental techniques [6, 10—12] while few works have been done on nonsteady laminar counterflow flames [13—17].

In the present article, we analyze the nonsteady behaviour of counterflow diffusion flames submitted to a time dependent injection velocities in the case of hydrogen — air flames using a detailed-kinetics numerical method and an experimental technique. The study is done for sinusoidal injection velocity variations, for moderate values and also for values near the extinction limit.

The experimental setup comprises two axisymmetric nozzles. This setup is issued from our previous works [12, 18] by adding two vibrating mechanisms in order to change the injection velocities. The amplitude and the frequency can easily be modified.

The OH emission intensity is used in our experiments to describe the flame response. It has been shown by different authors, by numerical and experimental studies of the flame structure, that the OH radical properly describes the evolution of the flame. Also, the spectroscopy of this radical is now well known. The measurements have been done in two different ways; first, from a global point of view, by detecting the total OH emission from the flame and second, from a more local point of view, the detection system being focused on the vertical axis and measuring single-line OH emission.

Experimental Setup

The experimental setup comprises two axisymmetric nozzles fixed on a vertical structure. Each burner features two concentric jets. The internal jet conveys the reactants while the surrounding nitrogen jet acts as an aerodynamic screen preventing the formation of a diffusion flame between the reactants and the ambient air. The diameters of the nozzles are respectively 20 mm (internal jet) and 40 mm (external jet). The distance h between the two burners may be varied but will be kept fixed in the present experiment ($h = 20$ mm). The lower burner may be moved in the horizontal plane in order to align the nozzle central axis. The two burners, including the berth, may be displaced in the radial and vertical directions to explore the whole flame zone without moving the optics or diagnostics. The translations are computer controlled with two stepping motors. This design is well suited to laser diagnostic measurements because the optical instrumentation is held fixed on a modular structure surrounding the combustor. This structure is placed on a heavy steel table fastened to a concrete block thus limiting the vibration level. The combustor design is also fully independent from the gas flow control system. Different reactant supply configurations may be used allowing both premixed and non-premixed flame operations. The upper and lower burners are fed with separate lines. For the most general use, each burner is supplied with nitrogen, oxygen and a fuel gas all stored in 200 bar reservoirs. A nitrogen flow creates an aerodynamic screen around each jet. Flow rates are measured by sonic nozzles and a large range of operating conditions may be covered by changing the sonic nozzle diameters. The flow control system comprises eight pressure measurement points which deliver pressure signals to a computer through an AD converter. The gas mixture is prepared in two separate chambers located on the downstream side of the sonic nozzles. More details on components used in the setup are given in [18, 19].

Each burner has a vibrating mechanism allowing injection velocity variations. This mechanism comprises a piston vibrating with the help of an actuator. The signal supplied to the actuator may have different shapes making possible different forms of piston vibrations. In the following experiments, the signal applied to each vibrating system is sinusoidal. A delay line is used to ensure a good phase concordance between the inlet velocities of the two injectors.

Two detection systems were used to get the flame response. The first system comprises a photomultiplier with an OH filter with maximum transmissivity corresponding to a wave-length of 307.1 nm. The emission from the whole flame disc is detected by this photomultiplier. The second system is a UV spectrometer coupled to a photomultiplier. It makes possible detecting one single emission line at a given wavelength from the OH radical. The spectrometer with an adequate optical configuration allows to focus on the region centered around the vertical axis of the flame. However, this second system gives a much smaller signal than the first one. The results presented here were obtained with the first system.

Governing Equations

A low-Mach number nonsteady laminar counterflow flame is considered. The governing equations along the stagnation streamline, using boundary-layer approximation and neglecting radiative heat transfer and external forces, and assuming a constant radial pressure gradient $\frac{1}{r}\frac{\partial p}{\partial r} = J$ along the axial coordinate [20, 21]. may be written in the following form:

$$\frac{\partial \rho}{\partial t} + (1 + j)\rho U + \frac{\partial (\rho v)}{\partial y} = 0, \tag{1}$$

$$\rho \frac{\partial U}{\partial t} + \rho U^2 + \rho v \frac{\partial U}{\partial y} + J - \frac{\partial}{\partial y}\left(\mu \frac{\partial U}{\partial y}\right) = 0, \tag{2}$$

$$\rho \frac{\partial Y_k}{\partial t} + \rho v \frac{\partial Y_k}{\partial y} + \frac{\partial}{\partial y}(\rho Y_k V_{ky}) - W_k \omega_k = 0. \quad k = 1, \ldots, K, \tag{3}$$

$$\rho c_p \frac{\partial T}{\partial t} + \rho v c_p \frac{\partial T}{\partial y} + \frac{\partial}{\partial y}\left(\lambda \frac{\partial T}{\partial y}\right) + \left(\sum_{k=1}^{K} \rho Y_k V_{ky} c_{pk}\right) \frac{\partial T}{\partial y} + \sum_{k=1}^{k} (h_k W_k \omega_k) = 0, \tag{4}$$

$$\frac{\partial J}{\partial y} = 0. \tag{5}$$

In these equations the mass density ρ, the temperature T and species mass fraction Y_k are only functions of the spatial coordinate normal to the stagnation plane y and the time t. U describes the y-dependence of the radial velocity u ($u = rU(y)$) and v denotes the axial velocity; μ denotes the local mixture viscosity; K, the number of species; V_{ky}, the diffusion velocity of the k^{th} species in the normal direction; W_k, the molecular weight of the k^{th} species; ω_k, the molar rate of production of the k^{th} species; λ, the local thermal conductivity of the mixture; c_p, the local constant pressure heat capacity of the mixture; c_{pk}, the constant pressure heat capacity of the k^{th} species; h_k, the specific enthalpy of the k^{th} species. The parameter j is equal to 0 or 1 for planar or axisymmetrical configuration respectively. The boundary conditions which complete this system of equations are as follows: at the lower nozzle ($y = y_L$): $U = 0$, $v = v_L$, $Y_k = Y_{kL}$, $k - 1, \ldots, K$ and $T = T_L$, at the upper nozzle ($y = y_U$): $U = 0$, $v = v_U$, $Y_k = Y_{kU}$, $k = 1, \ldots, K$ and $T = T_U$. In the present work we consider time dependent injection velocities ($v_L(t)$, $v_U(t)$). Hereafter, by «injection velocity variation» we mean that when $v_L(t)$ varies, $v_U(t)$ varies in phase with v_L so that $\rho_L v_L / \rho_U v_U$ remains constant at each instant.

The system of equations is completed by specifying the ideal-gas equation, the transport coefficients λ and μ, the diffusion velocities V_{ky}, the thermodynamic properties c_p, c_{pk} and h_k and the chemical production rates ω_k in terms of the state variables and their gradients. These expressions, which involve detailed transport and complex chemical kinetics, can be found in [22, 23].

The system of equations may be discretized and solved by a Linear Multistep Method [16, 24]. Lastly, we use vectorized versions of the CHEMKIN and TRANSPORT packages to evaluate transport coefficients and thermochemistry quantities [25].

Results

A large number of experiments and calculations has been done in the case of H_2/Air laminar counterflow diffusion flames. Here we give only a typical flame response to velocity fluctuations (Fig. 1). The experiment is done at atmospheric pressure. At the upper injector, the average air mass flow rate is $\dot{m}_{air} = 3.45 \cdot 10^{-1}$ g/s and its temperature is $T_{air} = 300$ K ($v_U = 1.0$ m/s). At the lower injector, the average H_2 mass flow rate is $\dot{m}_{H_2} = 4.6 \cdot 10^{-3}$ g/s and the average N_2 mass flow rate is $\dot{m}_{N_2} = 3.4 \cdot 10^{-1}$ g/s and the temperature is 300 K ($v_L = 1.33$ m/s). The equivalence ratio in this case is then equal to $\varnothing = 0.458$. The injection velocities fluctuate with a frequency of 40 Hz. Figure 1 represents the variation of normalized total OH emission of the flame as a function of time. The reference value for the normalization is that of a flame without velocity fluctuations. The OH response curve is slightly nonlinear. The noise signal has a frequency of about 1000 Hz and does not perturbate the OH signal. It remains the same at different velocity fluctuation frequencies.

A detailed reaction mechanism due to Warnatz, involving 9 species and 19 chemical reactions, is used to study the counterflow hydrogen — air

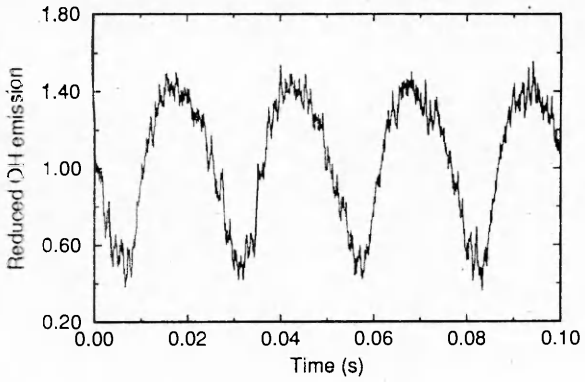

Fig. 1. Typical experimental flame response to injection velocity fluctuations; variation in time of reduced total OH emission intensity for $Y_{O2_U} = 0.233$ and $Y_{H2_L} = 0.0133$ ($\varnothing = 0.458$) with average injection velocities of $v_U = 1$ m/s and $v_L = 1.33$ m/s.

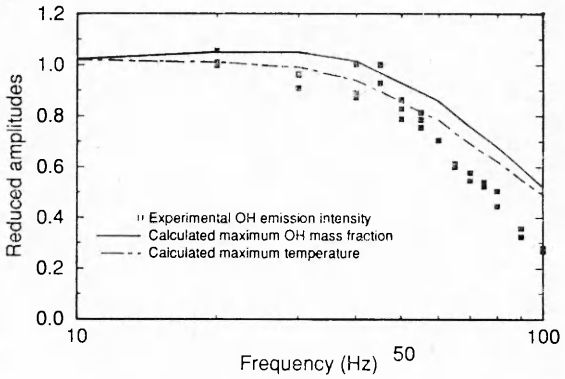

Fig. 2. Amplitude ratios of experimental OH emission intensity, calculated maximum OH mass fraction and calculated maximum temperature plotted as a function of frequency for $Y_{O2_U} = 0.233$ and $Y_{H2_L} = 0.0133$ ($\varnothing = 0.458$) with average injection velocities of $v_U = 1$ m/s and $v_L = 1.33$ m/s.

diffusion flames (see [16] for the reactions and species). All the calculations presented here have been done at the above experimental conditions.

Figure 2 shows the variation of the amplitude ratio of the calculated maximum temperature and maximum OH mass fraction and measured total OH emission as a function of the frequency. The amplitude ratio of each parameter X is calculated by $(X_{max} - X_{min})/(X_2 - X_1)$ in an established period. The subscript 1 refers to the value of the parameter X in a steady state flame with the injection velocities equal to the minimum values in a period of fluctuations. The subscript 2 refers to the value of the parameter X in a steady state flame with the injection velocities equal to the maximum values in a period of fluctuations. For small frequencies the amplitude ratio approaches unity. When the frequency increases the amplitude ratios become slightly greater than unity and then decrease. For high frequencies the amplitude ratios are small and one may consider that the flame does not respond to the oscillations of the flow. Far from the extinction limit, the flame response is observed to be linear.

The comparison between the numerical and experimental results shows a good concordance at low frequencies up to 50 Hz. The difference between the predicted and measured cut-off frequencies is probably due to pressure term J in the momentum equation. Another reason for this difference is that the calculations give the amplitude ratios on the axis of the jets while the measurements give the total OH emission corresponding to the whole flame disc emission. In fact, we have observed that at low frequencies, the extremity of the flame disc was naturally convected and moved up, but at high frequencies the flame disc diameter becomes smaller. As a consequence, at high frequencies, the amplitude of the total OH emission decreases more than the amplitude of the OH emission at the center of the flame disc.

The flame response near the extinction limit was deduced from calculations. The velocity fluctuations amplitude is such that the inlet veloci-

ties may exceed the velocity corresponding to extinction, but the average velocity remains smaller than this one. While far from the extinction limit the flame response is practically linear, it becomes strongly nonlinear near this limit. One also observes that at high frequencies the excursion time in the velocities beyond the critical conditions of extinction is sufficiently low and the flame does not have enough time to extinguish. The flame is insensitive to flow oscillations. At low frequencies, the excursion time becomes sufficiently long and the flame may be completely extinguished. The frequency corresponding to this extinction timit depends on the average injection velocity and its fluctuation amplitude.

Conclusion

In this article, we have analyzed the nonsteady behaviour of laminar hydrogen — air counterflow diffusion flames submitted to time dependent injection velocities using a complex-kinetics numerical method and an experimental technique. The study has been done for sinusoidal injection velocity variations.

Flames submitted to sinusoidal variations around a mean injection velocity exhibit a number of interesting features. Far from the extinction limit, the flame response is essentially linear. For small frequencies, the amplitude ratios approach unity. When the frequency increases the amplitude ratio increases slightly and then decreases. For very high frequencies the amplitude ratios are very small and the flame becomes essentially insensitive to flow oscillations.

A comparison between the numerical and experimental results shows that the response of the OH radical properly describes the evolution of the flame.

REFERENCES

1. **Libby P. A., Linan, Williams F. A.** Strained premixed laminar flames with nonunity Lewis numbers // Combust. Sci. and Technol.— 1983.— 34.— P. 257.
2. **Smooke M. D., Puri I. K., Seshadri K.** A comparison between numerical calculations and experimental measurements of the structure of a counterflow diffusion flame burning diluted methane in diluted air // 21st Symp. (Int.) on Combust., Reinhold, 1986.
3. **Giovangigli V., Smook M. D.** Extinction of strained premixed laminar flames with complex chemistry // Combust. Sci. and Technol.— 1987.— 53.— P. 23.
4. **Dixon-Lewis G., Missaghi.** Structure and extinction limits of counterflow diffusion flames of hydrogen — nitrogen mixture in air // 22nd Symp. (Int.) on Combust., The Combust. Inst., 1988.— P. 1461—1470.
5. **Seshadri K., Peters N.** Asymptotic structure and extinction of methane — air diffusion flames // Combust. Flame.— 1988.— 73.— P. 23.
6. **Law C. K.** Dynamics of stretched flames // 22nd Symp. (Int.) on Combust., The Combust. Inst., 1988.— P. 1381—1402.
7. **Rogg B.** Response and flamelet structure of stretched premixed methane — air flames // Combust. Flame.— 1988.— 73.— P. 45—65.
8. **Darabiha N., Giovangigli V., Candel S. et al.** Extinction of strained premixed propane — air flames with complex chemistry // Combust. Sci. and Technol.— 1988.— 60.— P. 267—285.
9. **Darabiha N., Candel S.** The influence of the temperature on extinction and ignition limits of strained hydrogen — air diffusion flames. To appear in Combust. Sci. and Technol., 1991.
10. **Ishizuka S., Law C. K.** An experimental study on extinction and stability of stretched premixed flames // 19th Symp. (Int.) on Combust., Reinhold, 1982.— P. 327.
11. **Tsuji H.** The influence of laminar transport and chemical kinetics on the time mean reaction rate in a turbulent flame // Progr. Eng. and Combust. Sci.— 1982.— 8.— P. 93.
12. **Rolon J. C., Veynante D., Martin J. P. et al.** Counter jet stagnation flows // Experiments in Fluids.— 1991.— 11.— P. 313—324.
13. **Carrier G. F., Fendell F. E., Marble F. E.** The effect of strain rate on diffusion flames // SIAM J. Appl. Math.— 1975.— 28.— P. 463.
14. **Linan A., Crespo A.** An asymptotic analysis of unsteady diffusion flames for large activation energies // Combust. Sci. and Technol.— 1976.— 14.— P. 95—117.
15. **Rogg B.** Numerical modeling and computation of reactive stagnation-point flows // Computer and Experiments in Fluid Flow.— 1989.— 75. Carlomagno G. M., Bredbia C. A. (Eds.), Springer Verlag, Berlin — Heidelberg, 1989.

16. **Darabiha N.** Transient behaviour of laminar counterflow hydrogen — air diffusion flames with complex chemistry. To appear in Combust. Sci. and Technol., 1991.
17. **Stahl G., Warnatz J.** Numerical investigation of time-dependent properties and extinction of strained methane — and propane — air flamelets // Combust. Flames.— 1991.— 85.— P. 285—299.
18. **Rolon J. C.** PhD thesis. Theoretical and experimental study of a counterflow diffusion flame. Ecole Centrale Paris, 1988.
19. **Djavdan E.** PhD thesis. Theoretical and experimental study of strained laminar premixed propane — air flames. Ecole Centrale Paris, 1990.
20. **Kee R. J., Miller J. A., Evans G. H. et al.** A computational model of the structure and extinction of strained, opposed flow, premixed methane — air flames // 22nd Symp. (Int.) on Combust., The Combust. Inst., 1988.— P. 1479—1494.
21. **Smooke M. D., Crump J., Seshadri K. et al.** Comparison between experimental measurements and numerical calculations of the structure of counterflow, diluted, methane — air premixed flames. Yale Univ. Report. ME—100—90.— 1990.
22. **Kee R. J., Miller J. A., Jefferson T. H.** CHEMKIN: A general-purpose, transportable, Fortran chemical kinetics code package. Sandia National Lab. Report, SAND80-8003.— 1980.
23. **Kee R. J., Warnatz J., Miller J. A.** A Fortran computer code package for the evaluation of gas-phase viscosities, conductivities, and diffusion coefficients. Sandia National Lab. Report, SAND83-8209.— 1983.
24. **Warming R. F., Beam R. M.** An extension of A-stability to alternating direction implicit methods. BIT — 1979.— 19.— P. 395—417.
25. **Darabiha N., Giovangigli V.** Vectorized computation of complex chemistry flames // Proc. of Int. Symp. on High Performance Computing/L. Delhaye and E. Gelenbe (Eds.).— Elsevier Sci. Publ. B. V. (North Holland), 1989.

УДК 621.452.226

R. F. Walter

RECENT ADVANCES IN COMPUTATIONAL ANALYSIS OF HYPERSONIC VEHICLES

W. J. Schafer Associates, Inc.
Albuquerque, New Mexico
USA

Abstract

The nonequilibrium gasdynamics processes of importance to hypersonic aerobraking vehicles are reviewed. Recent improvements in understanding these phenomena and in the detailed numerical modeling of these processes will be discussed. The paper concludes by describing the extent to which these models have been incorporated into multidimensional computational fluid dynamics (CFD) computer codes.

Physical Gasdynamics
Processes in the aerobraking environment

The chemistry and radiation processes which determine the heat transfer and aerodynamic force characteristics of aerobraking vehicles have been described in a series of excellent review papers [1—4]. Recently these considerations were extended to include the specific flight environments of manned missions to Mars, which employ aerobraking in both the Earth and the Martian atmospheres. Briefly, the one novel aspect of the AOTV flight environment when compared to those encountered by previous reentry systems such as Apollo; Soyuz, or the Space Shuttle Orbiter is the importance of nonequilibrium radiation in determining the heat transfer. This arises from the fact that the aerobraking vehicles will accomplish the required deceleration over a relatively long period of time (hundreds of seconds at high altitudes (70—100 km), whereas the Apollo spacecraft experienced peak heating and deceleration over a much shorter time (15 sec) at lower altitudes. This resulted in a situation whereby convective heat transfer dominated the thermal loads for Apollo. In contrast, the large phy-